

Josephson Transport across T-shaped and Series-Configured Double Quantum Dots System at Infinite-U Limit

Bhupendra Kumar ^{*}, Sachin Verma [†], Tanuj Chamoli [‡] and Ajay [§]

Department of Physics, Indian Institute of Technology Roorkee, 247667, Uttarakhand, India

August 21, 2023

Abstract

The charge transport has been analyzed theoretically across a T-shaped and series-configured double quantum dots Josephson junction by implementing the Slave Boson mean field approximation at an infinite-U limit. It has been shown that Andreev Bound states (ABS) and Josephson current can be tuned by varying the interdot tunneling (t) and quantum dots energy level. For the T-shape configuration of the quantum dots, an extra path is available for the transport of electrons which causes the interference destruction between two paths. For decoupled quantum dots with $\epsilon_{d1} = \epsilon_{d2} = 0$, the energy of ABS crosses at $\omega = 0$ and Josephson current shows a discontinuity at $\phi = \pm\pi$. On the other hand, for coupled quantum dots the lower and upper ABS has a finite spacing, the Josephson current exhibits sinusoidal nature and its magnitude suppresses with increasing interdot tunneling strength. While in the series configuration, with increment in t , Josephson current increases and shows a discontinuity at $\phi = \pm\pi$, once the system gets resonant tunneling for $t = 0.5\Gamma$ with $\epsilon_{d1} = \epsilon_{d2} = 0.5\Gamma$. Further, we also analyze the nature of the energy of ABS and Josephson current with the quantum dots energy level in both configurations.

Keywords: Josephson transport, quantum dots, Infinite-U Slave Boson mean field approximation.

I. INTRODUCTION

The Josephson effect is responsible for Cooper pair transport between two superconducting leads. It is the phase difference between two superconductors that lead to current flow; the sign of the current determines whether the state is called 0-phase or π -phase [1, 2]. Josephson effect studies are interesting when an insulator is replaced by quantum dots in the junction, where Josephson current flows due to the formation of subgap states i.e. Andreev Bound states (ABS). The energy level of quantum dots can be tuned by the gate voltage [3, 4]. In a superconductor-quantum dot system, the Andreev reflection process occurs at the interfaces between the quantum dot and the superconducting leads. In this process, an electron from one of the leads strikes the dot, it can be retro-reflected as a hole, forming a Cooper pair in the superconducting lead. The existence of Andreev Bound states may significantly affect the system's transport characteristics. They have the potential to cause resonant tunneling as well as the creation of conductance peaks in the tunneling spectrum. Additionally, Andreev bound states can be utilized to design innovative quantum devices, such as qubits for quantum computing and superconducting nanoelectronics. A thorough overview of quantum dot-superconductor systems is provided in reference [5, 6], which also includes studies of Andreev bound states and Josephson supercurrent in previous years [7–27].

It has been an active research topic in recent years to study quantum electronic transport across systems where double quantum dots are linked to superconducting leads, because of the tunable parameters such as energy levels of quantum dots, dot-lead coupling strength, and interdot tunneling. The inter-

dot tunneling decides whether the dots are strongly or weakly coupled. These controlling tunable parameters of DQD make it helpful to analyze the transport phenomena like the Coulomb blockade, Kondo effect, quantum coherence, etc. A double quantum dot (DQD) system can be configured in three different ways: serially, T-shaped, or parallelly [28–30]. There are number of theoretical studies addressing the Josephson current when coupled double quantum dots are connected to BCS superconducting lead at finite on-dot Coulomb interactions (U) [31–36]. In these theoretical studies, techniques such as non-equilibrium Green's function method [37, 38], quantum Monte Carlo simulation [39], perturbation theory [40], and renormalization group method have been used [41–46]. S-DQD-S systems have been formed through various experimental techniques [47–52]. The subgap gap states and Josephson current are also investigated at a very strong Coulomb correlation i.e. U is quite large in comparison to the other energy scales, Δ , and interdot tunneling (t) and energy levels of quantum dots, in some research works [46, 53–55]. Our assumption that on-dot Coulomb repulsion is infinite is supported by this observation. Due to the infinite on-dot Coulomb interaction $U \rightarrow \infty$, both quantum dots, QD_1 and QD_2 , are singly occupied.

In the present research work, we have applied Slave Boson mean-field approximation [29, 56–62] to study the Andreev Bound states and Josephson current through a T-shaped and series-configured double quantum dots Josephson junction. In T-shape configuration, QD_1 is directly coupled with superconducting leads, and QD_2 is only coupled with the QD_1 (figure 1a). In a series configuration, QD_1 is coupled with the left

*bhupendra_k@ph.iitr.ac.in

†sverma2@ph.iitr.ac.in

‡tchamoli@ph.iitr.ac.in

§ajay@ph.iitr.ac.in

superconducting lead, and QD_2 is linked with the right superconducting lead (figure 1b). This infinite-U technique is sus-

tainable for conditions where $T_K > \Delta$ where T_K is the Kondo temperature and Δ is the Cooper pair binding energy [63, 64].

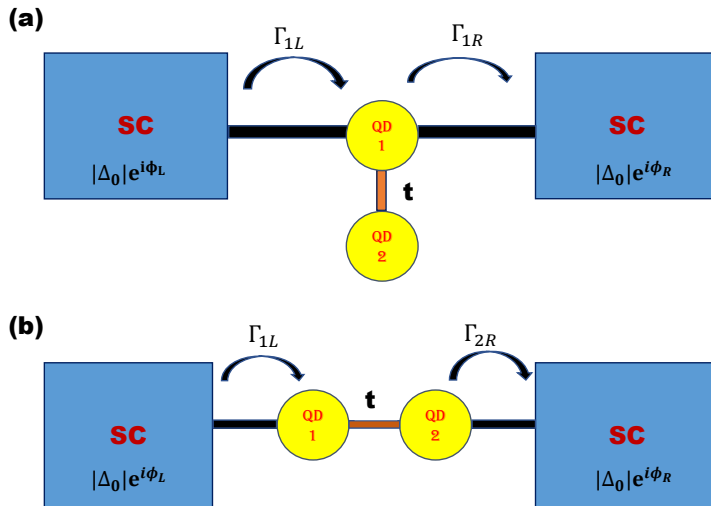


Figure 1: A schematic picture of a system with double quantum dots in (a) T-shape geometry and (b) series geometry connected to two superconducting leads with phase ϕ_α where $\alpha \in L, R$.

II. THEORETICAL FORMULATION

The double quantum dots system in T-shaped and in series configuration is modeled by generalized Anderson and BCS Hamiltonian in second quantization formalism as follows:

[A]: T-shaped configuration:

$$\hat{H} = \hat{H}_{leads} + \hat{H}_{dots} + \hat{H}_{interdot-tunneling} + \hat{H}_{dot-lead} \quad (1)$$

where

$$\hat{H}_{leads} = \sum_{k\sigma,\alpha} \epsilon_{k\alpha} c_{k\sigma,\alpha}^\dagger c_{k\sigma,\alpha} - \left(\sum_{k\alpha} \Delta_\alpha c_{k\uparrow,\alpha}^\dagger c_{-k\downarrow,\alpha}^\dagger + h.c. \right)$$

$$\hat{H}_{dots} = \sum_{i\sigma} \epsilon_{d_i} d_{i\sigma}^\dagger d_{i\sigma} + \sum_{i\sigma} U_i n_{i\sigma} n_{i\bar{\sigma}} + U_{12} n_1 n_2$$

$$\hat{H}_{interdot-tunneling} = \sum_{i\sigma} t d_{1\sigma}^\dagger d_{2\sigma} + h.c.$$

$$\hat{H}_{dot-lead} = \sum_{k\sigma,\alpha} h_{1k,\alpha} c_{k\sigma,\alpha}^\dagger d_{1\sigma} + h.c.$$

\hat{H}_{leads} is the Hamiltonian of BCS superconducting leads. In the first term $\epsilon_{k\alpha}$ is the energy of superconducting leads ($\alpha \in L, R$) and $c_{k\sigma,\alpha}^\dagger$ ($c_{k\sigma,\alpha}$) is the creation (annihilation) operator of electrons with spin σ (\uparrow, \downarrow) and wave vector \vec{k} . The second term denotes the interaction between Cooper pairs where Δ_α is the superconducting order parameter and is given as $\Delta_\alpha = |\Delta_0| e^{i\phi_\alpha}$.

\hat{H}_{dots} denotes the Hamiltonian of double quantum dots. The energy of main quantum dot (QD_1) and side quantum dot (QD_2) is given by ϵ_{d_i} with fermionic operators ($d_{i\sigma}^\dagger$ and $d_{i\sigma}$). U_1, U_2 are Coulomb interactions on QD_1 and QD_2 respectively. U_{12} is the intra-dot Coulomb interaction.

$\hat{H}_{interdot-tunneling}$ is the Hamiltonian for tunneling between both quantum dots and the amplitude of interdot tunneling is symbolized by t .

$\hat{H}_{dot-lead}$ represents the hamiltonian for tunneling between QD_1 and superconducting leads where $h_{1k,\alpha}$ is the tunneling strength between leads and QD_1 .

The Bogoliubov transformation is used to obtain the diagonalized Hamiltonian.

$$c_{k\uparrow,\alpha} = u_{k\alpha}^* \beta_{k\uparrow,\alpha} + v_{k\alpha} \beta_{-k\downarrow,\alpha}^\dagger \quad (2)$$

$$c_{k\downarrow,\alpha} = u_{k\alpha}^* \beta_{k\downarrow,\alpha} - v_{k\alpha} \beta_{-k\uparrow,\alpha}^\dagger \quad (3)$$

$$c_{k\uparrow,\alpha}^\dagger = u_{k\alpha} \beta_{k\uparrow,\alpha}^\dagger + v_{k\alpha}^* \beta_{-k\downarrow,\alpha} \quad (4)$$

$$c_{k\downarrow,\alpha}^\dagger = u_{k\alpha} \beta_{k\downarrow,\alpha}^\dagger - v_{k\alpha}^* \beta_{-k\uparrow,\alpha} \quad (5)$$

After employing the above Bogoliubov transformation relations, the Hamiltonian can be expressed as:

$$\begin{aligned} \hat{H} = & \sum_{k\alpha} E_{k\alpha} (\beta_{k\uparrow,\alpha}^\dagger \beta_{k\uparrow,\alpha} + \beta_{-k\downarrow,\alpha}^\dagger \beta_{-k\downarrow,\alpha}) \\ & + \sum_{i\sigma} \epsilon_{d_i} d_{i\sigma}^\dagger d_{i\sigma} + \sum_{i\sigma} (t d_{1\sigma}^\dagger d_{2\sigma} + t^* d_{2\sigma}^\dagger d_{1\sigma}) \\ & + \sum_{i\sigma} U_i n_{i\sigma} n_{i\bar{\sigma}} + U_{12} n_1 n_2 \\ & + \sum_{k\sigma} h_{1k,\alpha} [(u_{k\alpha} \beta_{k\uparrow,\alpha}^\dagger + v_{k\alpha}^* \beta_{-k\downarrow,\alpha}) d_{1\uparrow} \\ & + (u_{k\alpha} \beta_{k\uparrow,\alpha}^\dagger - v_{k\alpha}^* \beta_{-k\uparrow,\alpha}) d_{1\downarrow}] \\ & + \sum_{k\sigma} h_{1k,\alpha} [d_{1\uparrow}^\dagger (u_{k\alpha}^* \beta_{k\uparrow,\alpha} + v_{k\alpha} \beta_{-k\downarrow,\alpha}^\dagger) \\ & + d_{1\downarrow}^\dagger (u_{k\alpha}^* \beta_{k\downarrow,\alpha} - v_{k\alpha} \beta_{-k\uparrow,\alpha}^\dagger)] \end{aligned} \quad (6)$$

where

$$E_{k\alpha} = \sqrt{\epsilon_{k\alpha}^2 + |\Delta_{k\alpha}^2|} \quad (7)$$

$$\begin{aligned}
|u_{k\alpha}^2| &= \frac{1}{2} \left(1 + \frac{\epsilon_{k\alpha}}{\sqrt{\epsilon_{k\alpha}^2 + |\Delta_{k\alpha}^2|}} \right) \\
|v_{k\alpha}^2| &= \frac{1}{2} \left(1 - \frac{\epsilon_{k\alpha}}{\sqrt{\epsilon_{k\alpha}^2 + |\Delta_{k\alpha}^2|}} \right) \\
u_{k\alpha}^* v_{k\alpha} &= \frac{\Delta_{k\alpha}}{2E_{k\alpha}} \\
v_{k\alpha}^* u_{k\alpha} &= \frac{\Delta_{k\alpha}^*}{2E_{k\alpha}}
\end{aligned} \tag{8}$$

To study the Andreev Bound states and supercurrent at infinite-U limit ($U_i \rightarrow \infty$), we introduce the fermionic operators $f_{i\sigma}^\dagger$ and $f_{i\sigma}$ in terms of bosonic operators b_i^\dagger and b_i .

$$d_{i\sigma} = b_i^\dagger f_{i\sigma}, d_{i\sigma}^\dagger = f_{i\sigma}^\dagger b_i \tag{9}$$

Here, $f_{i\sigma}$ denotes the singly occupied states and b denotes the empty dot states. There are two quantum dots in our system therefore to apply the Infinite-U Slave Boson approximation approach, we have to introduce two Lagrange multipliers λ_1 and λ_2 to force the constraint in this fashion.

$$b_i^\dagger b_i + \sum_{\sigma} f_{i\sigma}^\dagger f_{i\sigma} = 1 \tag{10}$$

For simplicity, we have neglected the intra-dot Coulomb repulsion U_{12} because it is small as compared to other energy parameters. Finally, in the infinite-U limit, the effective Slave Boson mean field Hamiltonian with $\langle b_i^\dagger(t) \rangle = \langle b_i(t) \rangle = b_i$ can be expressed as:

$$\begin{aligned}
\hat{H}_{SBMF} &= \sum_{k\alpha} E_{k\alpha} (\beta_{k\uparrow,\alpha}^\dagger \beta_{k\uparrow,\alpha} + \beta_{-k\downarrow,\alpha}^\dagger \beta_{-k\downarrow,\alpha}) \\
&+ \sum_{i\sigma} \tilde{\epsilon}_{di} f_{i\sigma}^\dagger f_{i\sigma} + \sum_{i\sigma} (\tilde{t} f_{1\sigma}^\dagger f_{2\sigma} + \tilde{t}^* f_{2\sigma}^\dagger f_{1\sigma}) \\
&+ \sum_{k\sigma} \tilde{h}_{1k,\alpha} [(u_{k\alpha} \beta_{k\uparrow,\alpha}^\dagger + v_{k\alpha}^* \beta_{-k\downarrow,\alpha}) f_{1\uparrow} \\
&+ (u_{k\alpha} \beta_{k\uparrow,\alpha}^\dagger - v_{k\alpha}^* \beta_{-k\uparrow,\alpha}) f_{1\downarrow}] \\
&+ \sum_{k\sigma} \tilde{h}_{1k,\alpha}^* [f_{1\uparrow}^\dagger (u_{k\alpha}^* \beta_{k\uparrow,\alpha} + v_{k\alpha} \beta_{-k\downarrow,\alpha}^\dagger) \\
&+ f_{1\downarrow}^\dagger (u_{k\alpha}^* \beta_{k\downarrow,\alpha} - v_{k\alpha} \beta_{-k\uparrow,\alpha}^\dagger)] \\
&+ \lambda_1 (b_1^2 - 1) + \lambda_2 (b_2^2 - 1)
\end{aligned} \tag{11}$$

where $\tilde{\epsilon}_{di}$ are renormalized energy levels of quantum dots, \tilde{t} is the renormalized interdot tunneling strength, and $\tilde{h}_{1k,\alpha}$ is the renormalized dot lead tunneling strength, and can be written as:

$$\begin{aligned}
\tilde{h}_{1k,\alpha} &= b_1 h_{1k,\alpha} \\
\tilde{\epsilon}_{di} &= \epsilon_{di} + \lambda_i \\
\tilde{t} &= t b_1 b_2
\end{aligned} \tag{12}$$

Based on Green's equation of motion technique, the following closed-coupled equations are obtained.

$$\begin{aligned}
(\omega - \tilde{\epsilon}_{d1}) \langle \langle f_{1\uparrow} | f_{1\uparrow}^\dagger \rangle \rangle &= 1 + \sum_{k\alpha} \tilde{h}_{1k,\alpha}^* u_{k\alpha}^* \langle \langle \beta_{k\uparrow,\alpha} | f_{1\uparrow}^\dagger \rangle \rangle \\
&+ \sum_{k\alpha} \tilde{h}_{1k,\alpha}^* v_{k\alpha} \langle \langle \beta_{-k\downarrow,\alpha} | f_{1\uparrow}^\dagger \rangle \rangle \\
&+ \tilde{t} \langle \langle f_{2\uparrow} | f_{1\uparrow}^\dagger \rangle \rangle
\end{aligned} \tag{13}$$

$$\begin{aligned}
(\omega - E_{k\alpha}) \langle \langle \beta_{k\uparrow,\alpha} | f_{1\uparrow}^\dagger \rangle \rangle &= \sum_{k\alpha} \tilde{h}_{1k,\alpha} u_{k\alpha} \langle \langle f_{1\uparrow} | f_{1\uparrow}^\dagger \rangle \rangle \\
&+ \sum_{k\alpha} \tilde{h}_{1k,\alpha}^* v_{k\alpha} \langle \langle f_{1\downarrow} | f_{1\uparrow}^\dagger \rangle \rangle
\end{aligned} \tag{14}$$

$$\begin{aligned}
(\omega + E_{k\alpha}) \langle \langle \beta_{-k\downarrow,\alpha} | f_{1\uparrow}^\dagger \rangle \rangle &= \sum_{k\alpha} \tilde{h}_{1k,\alpha} v_{k\alpha}^* \langle \langle f_{1\uparrow} | f_{1\uparrow}^\dagger \rangle \rangle \\
&- \sum_{k\alpha} \tilde{h}_{1k,\alpha}^* u_{k\alpha}^* \langle \langle f_{1\downarrow} | f_{1\uparrow}^\dagger \rangle \rangle
\end{aligned} \tag{15}$$

$$\begin{aligned}
(\omega + \tilde{\epsilon}_{d1}) \langle \langle f_{1\downarrow} | f_{1\uparrow}^\dagger \rangle \rangle &= \sum_{k\alpha} \tilde{h}_{1k,\alpha} v_{k\alpha}^* \langle \langle \beta_{-k\uparrow,\alpha} | f_{1\uparrow}^\dagger \rangle \rangle \\
&- \sum_{k\alpha} \tilde{h}_{1k,\alpha} u_{k\alpha} \langle \langle \beta_{k\downarrow,\alpha} | f_{1\uparrow}^\dagger \rangle \rangle \\
&- \tilde{t}^* \langle \langle f_{2\downarrow} | f_{1\uparrow}^\dagger \rangle \rangle
\end{aligned} \tag{16}$$

$$\begin{aligned}
(\omega - E_{k\alpha}) \langle \langle \beta_{-k\uparrow,\alpha} | f_{1\uparrow}^\dagger \rangle \rangle &= \sum_{k\alpha} \tilde{h}_{1k,\alpha} u_{k\alpha} \langle \langle f_{1\uparrow} | f_{1\uparrow}^\dagger \rangle \rangle \\
&+ \sum_{k\alpha} \tilde{h}_{1k,\alpha}^* v_{k\alpha} \langle \langle f_{1\downarrow} | f_{1\uparrow}^\dagger \rangle \rangle
\end{aligned} \tag{17}$$

$$\begin{aligned}
(\omega + E_{k\alpha}) \langle \langle \beta_{k\downarrow,\alpha} | f_{1\uparrow}^\dagger \rangle \rangle &= \sum_{k\alpha} \tilde{h}_{1k,\alpha} v_{k\alpha}^* \langle \langle f_{1\uparrow} | f_{1\uparrow}^\dagger \rangle \rangle \\
&- \sum_{k\alpha} \tilde{h}_{1k,\alpha}^* u_{k\alpha}^* \langle \langle f_{1\downarrow} | f_{1\uparrow}^\dagger \rangle \rangle
\end{aligned} \tag{18}$$

$$(\omega - \tilde{\epsilon}_{d2}) \langle \langle f_{1\uparrow} | f_{1\uparrow}^\dagger \rangle \rangle = \tilde{t}^* \langle \langle f_{1\uparrow} | f_{1\uparrow}^\dagger \rangle \rangle \tag{19}$$

$$(\omega + \tilde{\epsilon}_{d2}) \langle \langle f_{1\uparrow} | f_{1\uparrow}^\dagger \rangle \rangle = -\tilde{t} \langle \langle f_{1\downarrow} | f_{1\uparrow}^\dagger \rangle \rangle \tag{20}$$

After solving the set of closed-coupled equations (Eq.13-20), the single particle retarded Green's function for QD can be written as:

$$\begin{aligned}
G_{11} = \langle \langle f_{1\uparrow} | f_{1\uparrow}^\dagger \rangle \rangle &= \frac{1}{\omega - \tilde{\epsilon}_{d1} - \tilde{\zeta}_{2\alpha} - \frac{\tilde{t}^2}{\omega - \tilde{\epsilon}_{d2}} - \frac{\tilde{\zeta}_{3\alpha} \tilde{\zeta}_{4\alpha}}{\omega + \tilde{\epsilon}_{d1} - \frac{\tilde{t}^2}{\omega + \tilde{\epsilon}_{d2}} - \tilde{\zeta}_{1\alpha}}} \\
&= \frac{1}{\omega - \tilde{\epsilon}_{d1} - \tilde{\Lambda}}
\end{aligned} \tag{21}$$

where

$$\tilde{\Lambda} = \tilde{\zeta}_{2\alpha} + \frac{\tilde{t}^2}{\omega - \tilde{\epsilon}_{d2}} + \frac{\tilde{\zeta}_{3\alpha} \tilde{\zeta}_{4\alpha}}{\omega + \tilde{\epsilon}_{d1} - \frac{\tilde{t}^2}{\omega + \tilde{\epsilon}_{d2}} - \tilde{\zeta}_{1\alpha}} \tag{22}$$

and also

$$\begin{aligned}
\tilde{\zeta}_{1\alpha} &= \sum_{k\alpha} |\tilde{h}_{1k,\alpha}|^2 \left(\frac{|u_{k\alpha}|^2}{\omega + E_{k\alpha}} + \frac{|v_{k\alpha}|^2}{\omega - E_{k\alpha}} \right) \\
&= -i \frac{\tilde{\Gamma}_{1\alpha}}{2} \gamma_\alpha(\omega)
\end{aligned} \tag{23}$$

$$\begin{aligned}
\tilde{\zeta}_{2\alpha} &= \sum_{k\alpha} |\tilde{h}_{1k,\alpha}|^2 \left(\frac{|u_{k\alpha}|^2}{\omega - E_{k\alpha}} + \frac{|v_{k\alpha}|^2}{\omega + E_{k\alpha}} \right) \\
&= -i \frac{\tilde{\Gamma}_{1\alpha}}{2} \gamma_\alpha(\omega)
\end{aligned} \tag{24}$$

$$\begin{aligned}
\tilde{\zeta}_{3\alpha} &= \sum_{k\alpha} |\tilde{h}_{1k,\alpha}|^2 v_{k\alpha}^* u_{k\alpha} \left(\frac{1}{\omega - E_{k\alpha}} - \frac{1}{\omega + E_{k\alpha}} \right) \\
&= -i \frac{\tilde{\Gamma}_{1\alpha}}{2} \gamma_\alpha(\omega) \frac{\Delta^*}{\omega}
\end{aligned} \tag{25}$$

$$\begin{aligned}
\tilde{\zeta}_{4\alpha} &= \sum_{k\alpha} |\tilde{h}_{1k,\alpha}|^2 u_{k\alpha}^* v_{k\alpha} \left(\frac{1}{\omega - E_{k\alpha}} - \frac{1}{\omega + E_{k\alpha}} \right) \\
&= -i \frac{\tilde{\Gamma}_{1\alpha}}{2} \gamma_\alpha(\omega) \frac{\Delta}{\omega}
\end{aligned} \tag{26}$$

where $\tilde{\Gamma}_{1\alpha}$ represents the renormalized coupling strength between QD_1 and superconducting leads and defines as $\tilde{\Gamma}_{1\alpha} = |b_i|^2 \Gamma_{1\alpha}$. $\Gamma_{1\alpha} = 2\pi\gamma_\alpha |h_{1\alpha}|^2$ stands for coupling strength. The BCS superconducting density of states (γ_α) can be written as follows.

$$\gamma_\alpha(\omega) = \frac{\omega\theta(\Delta_\alpha - |\omega|)}{\sqrt{\Delta_\alpha^2 - \omega^2}} + i \frac{|\omega|\theta(|\omega| - \Delta_\alpha)}{\sqrt{\omega^2 - \Delta_\alpha^2}} \quad (27)$$

[B]: Series configuration:

$$\hat{H} = \hat{H}_{leads} + \hat{H}_{dots} + \hat{H}_{interdot-tunneling} + \hat{H}_{dot-lead} \quad (28)$$

where

$$\hat{H}_{leads} = \sum_{k\sigma} \epsilon_{kL} c_{k\sigma,L}^\dagger c_{k\sigma,L} + \sum_{k\sigma} \epsilon_{kR} c_{k\sigma,R}^\dagger c_{k\sigma,R} - \left(\sum_{k\alpha} \Delta_\alpha c_{k\uparrow,\alpha}^\dagger c_{-k\downarrow,\alpha}^\dagger + h.c. \right)$$

$$\hat{H}_{dots} = \sum_{i\sigma} \epsilon_{d_i} d_{i\sigma}^\dagger d_{i\sigma} + \sum_{i\sigma} U_i n_{i\sigma} n_{i\bar{\sigma}} + U_{12} n_1 n_2$$

$$\hat{H}_{interdot-tunneling} = \sum_{i\sigma} t d_{1\sigma}^\dagger d_{2\sigma} + h.c$$

$$\hat{H}_{dot-lead} = \sum_{k\sigma} \left(h_{1k,L} c_{k\sigma,L}^\dagger d_{1\sigma} + h_{2k,R} c_{k\sigma,R}^\dagger d_{2\sigma} \right) + h.c$$

Again, by employing the Bogoliubov transformation and introducing the fermionic operator, the effective Slave Boson mean field Hamiltonian can be expressed as:

$$\begin{aligned} \hat{H}_{SBMF} = & \sum_k E_{kL} (\beta_{k\uparrow,L}^\dagger \beta_{k\uparrow,L} + \beta_{-k\downarrow,L}^\dagger \beta_{-k\downarrow,L}) \\ & + \sum_k E_{kR} (\beta_{k\uparrow,R}^\dagger \beta_{k\uparrow,R} + \beta_{-k\downarrow,R}^\dagger \beta_{-k\downarrow,R}) \\ & + \sum_\sigma \tilde{\epsilon}_{d1} f_{1\sigma}^\dagger f_{1\sigma} + \sum_\sigma \tilde{\epsilon}_{d2} f_{2\sigma}^\dagger f_{2\sigma} \\ & + (\tilde{t} f_{1\sigma}^\dagger f_{2\sigma} + \tilde{t}^* f_{2\sigma}^\dagger f_{1\sigma}) \\ & + \sum_{k\sigma} \tilde{h}_{1k,L} [(u_{kL} \beta_{k\uparrow,L}^\dagger + v_{kL}^* \beta_{-k\downarrow,L}) f_{1\uparrow} \\ & + (u_{kL} \beta_{k\uparrow,L}^\dagger - v_{kL}^* \beta_{-k\uparrow,L}) f_{1\downarrow}] \\ & + \sum_{k\sigma} \tilde{h}_{1k,L}^* [f_{1\uparrow}^\dagger (u_{kL}^* \beta_{k\uparrow,L} + v_{kL} \beta_{-k\downarrow,L}^*) \\ & + f_{1\downarrow}^\dagger (u_{kL}^* \beta_{k\downarrow,L} - v_{kL} \beta_{-k\uparrow,L}^*)] \\ & + \sum_{k\sigma} \tilde{h}_{2k,R} [(u_{kR} \beta_{k\uparrow,R}^\dagger + v_{kR}^* \beta_{-k\downarrow,R}) f_{1\uparrow} \\ & + (u_{kR} \beta_{k\uparrow,R}^\dagger - v_{kR}^* \beta_{-k\uparrow,R}) f_{1\downarrow}] \\ & + \sum_{k\sigma} \tilde{h}_{2k,R}^* [f_{1\uparrow}^\dagger (u_{kR}^* \beta_{k\uparrow,R} + v_{kR} \beta_{-k\downarrow,R}^*) \\ & + f_{1\downarrow}^\dagger (u_{kR}^* \beta_{k\downarrow,R} - v_{kR} \beta_{-k\uparrow,R}^*)] \\ & + \lambda_1 (b_1^2 - 1) + \lambda_2 (b_2^2 - 1) \end{aligned} \quad (29)$$

Based on Green's equation of motion technique, the following closed-coupled equations are obtained for series configured double quantum dots coupled to superconducting leads.

$$\begin{aligned} (\omega - \tilde{\epsilon}_{d1}) \langle \langle f_{1\uparrow} | f_{1\uparrow}^\dagger \rangle \rangle = & 1 + \sum_k \tilde{h}_{1k,L}^* u_{kL}^* \langle \langle \beta_{k\uparrow,L} | f_{1\uparrow}^\dagger \rangle \rangle \\ & + \sum_k \tilde{h}_{1k,L} v_{kL} \langle \langle \beta_{-k\downarrow,L}^\dagger | f_{1\uparrow}^\dagger \rangle \rangle \\ & + \tilde{t} \langle \langle f_{2\uparrow} | f_{1\uparrow}^\dagger \rangle \rangle \end{aligned} \quad (30)$$

$$\begin{aligned} (\omega - E_{kL}) \langle \langle \beta_{k\uparrow,L} | f_{1\uparrow}^\dagger \rangle \rangle = & \sum_k \tilde{h}_{1k,L} u_k \langle \langle f_{1\uparrow} | f_{1\uparrow}^\dagger \rangle \rangle \\ & + \sum_k \tilde{h}_{1k,L}^* v_{kL} \langle \langle f_{1\downarrow}^\dagger | f_{1\uparrow}^\dagger \rangle \rangle \end{aligned} \quad (31)$$

$$\begin{aligned} (\omega + E_{kL}) \langle \langle \beta_{-k\downarrow,L}^\dagger | f_{1\uparrow}^\dagger \rangle \rangle = & \sum_k \tilde{h}_{1k,L} v_{kL}^* \langle \langle f_{1\uparrow} | f_{1\uparrow}^\dagger \rangle \rangle \\ & - \sum_k \tilde{h}_{1k,L}^* u_{kL}^* \langle \langle f_{1\downarrow}^\dagger | f_{1\uparrow}^\dagger \rangle \rangle \end{aligned} \quad (32)$$

$$\begin{aligned} (\omega + \tilde{\epsilon}_{d1}) \langle \langle f_{1\downarrow}^\dagger | f_{1\uparrow}^\dagger \rangle \rangle = & \sum_k \tilde{h}_{1k,L} v_{kL}^* \langle \langle \beta_{-k\uparrow,L} | f_{1\uparrow}^\dagger \rangle \rangle \\ & - \sum_k \tilde{h}_{1k,L} u_{kL} \langle \langle \beta_{k\downarrow,L}^\dagger | f_{1\uparrow}^\dagger \rangle \rangle \\ & - \tilde{t}^* \langle \langle f_{2\downarrow} | f_{1\uparrow}^\dagger \rangle \rangle \end{aligned} \quad (33)$$

$$\begin{aligned} (\omega - E_{kR}) \langle \langle \beta_{k\uparrow,R} | f_{1\uparrow}^\dagger \rangle \rangle = & \sum_k \tilde{h}_{2k,R} u_{k\alpha} \langle \langle f_{1\uparrow} | f_{1\uparrow}^\dagger \rangle \rangle \\ & + \sum_{k\alpha} \tilde{h}_{2k,R}^* v_{kR} \langle \langle f_{1\downarrow}^\dagger | f_{1\uparrow}^\dagger \rangle \rangle \end{aligned} \quad (34)$$

$$\begin{aligned} (\omega + E_{kR}) \langle \langle \beta_{-k\downarrow,R}^\dagger | f_{1\uparrow}^\dagger \rangle \rangle = & \sum_k \tilde{h}_{2k,R} v_{kR}^* \langle \langle f_{1\uparrow} | f_{1\uparrow}^\dagger \rangle \rangle \\ & - \sum_k \tilde{h}_{2k,R}^* u_{kR}^* \langle \langle f_{1\downarrow}^\dagger | f_{1\uparrow}^\dagger \rangle \rangle \end{aligned} \quad (35)$$

$$\begin{aligned} (\omega - \tilde{\epsilon}_{d2}) \langle \langle f_{2\uparrow} | f_{1\uparrow}^\dagger \rangle \rangle = & t \langle \langle f_{1\uparrow} | f_{1\uparrow}^\dagger \rangle \rangle \\ & + \tilde{h}_{2k,R} u_{kR}^* \langle \langle \beta_{k\uparrow,R} | f_{1\uparrow}^\dagger \rangle \rangle \\ & + \tilde{h}_{2k,R}^* v_{kR} \langle \langle \beta_{-k\downarrow,R}^\dagger | f_{1\uparrow}^\dagger \rangle \rangle \end{aligned} \quad (36)$$

$$\begin{aligned} (\omega + \tilde{\epsilon}_{d2}) \langle \langle f_{1\uparrow} | f_{1\uparrow}^\dagger \rangle \rangle = & -t \langle \langle f_{1\downarrow}^\dagger | f_{1\uparrow}^\dagger \rangle \rangle \\ & + \tilde{h}_{2k,R} v_{kR}^* \langle \langle \beta_{-k\uparrow,R} | f_{1\uparrow}^\dagger \rangle \rangle \\ & - \tilde{h}_{2k,R} u_{kR} \langle \langle \beta_{k\downarrow,R}^\dagger | f_{1\uparrow}^\dagger \rangle \rangle \end{aligned} \quad (37)$$

After solving the set of closed-coupled equations (Eq.30-Eq.37), the single particle retarded Green's function for QD can be written as:

$$G_{11} = \frac{1}{\omega - \tilde{\epsilon}_{d1} - \tilde{\Lambda}} \quad (38)$$

$$\tilde{\Lambda} = A - \frac{B \cdot C}{D}$$

where

$$A = \tilde{\zeta}_{1L}(2) + \frac{\tilde{t}^2}{\omega - \tilde{\epsilon}_{d2} - \tilde{\zeta}_{2R}(2) - \frac{\tilde{\zeta}_{3R}\tilde{\zeta}_{4R}}{\omega + \tilde{\epsilon}_{d2} - \tilde{\zeta}_{2R}(1)}}$$

$$B = \tilde{\zeta}_{4L} - \frac{\tilde{t}^2 \cdot \tilde{\zeta}_{4R}}{(\omega + \tilde{\epsilon}_{d2} - \tilde{\zeta}_{2R}(1))(\omega - \tilde{\epsilon}_{d2} - \tilde{\zeta}_{2R}(2) - \frac{\tilde{\zeta}_{3R}\tilde{\zeta}_{4R}}{\omega + \tilde{\epsilon}_{d2} - \tilde{\zeta}_{2R}(1)})}$$

$$C = \tilde{\zeta}_{3L} - \frac{\tilde{t}^2 \cdot \tilde{\zeta}_{3R}}{(\omega - \tilde{\epsilon}_{d2} - \tilde{\zeta}_{2R}(2))(\omega + \tilde{\epsilon}_{d2} - \tilde{\zeta}_{2R}(1) - \frac{\tilde{\zeta}_{3R}\tilde{\zeta}_{4R}}{\omega - \tilde{\epsilon}_{d2} - \tilde{\zeta}_{2R}(2)})}$$

$$D = \omega + \tilde{\epsilon}_{d1} - \tilde{\zeta}_{1L}(1) - \frac{\tilde{t}^2}{\omega + \tilde{\epsilon}_{d2} - \tilde{\zeta}_{2R}(1) - \frac{\tilde{\zeta}_{3R}\tilde{\zeta}_{4R}}{\omega - \tilde{\epsilon}_{d2} - \tilde{\zeta}_{2R}(2)}}$$

Also, where

$$\begin{aligned}\tilde{\zeta}_{1L}(1) &= \sum_k |\tilde{h}_{1k,L}|^2 \left(\frac{|u_{kL}|^2}{\omega + E_{kL}} + \frac{|v_{kL}|^2}{\omega - E_{kL}} \right) \\ &= -i \frac{\tilde{\Gamma}_{1L}}{2} \gamma_L(\omega)\end{aligned}\quad (39)$$

$$\begin{aligned}\tilde{\zeta}_{1L}(2) &= \sum_k |\tilde{h}_{1k,L}|^2 \left(\frac{|u_{kL}|^2}{\omega - E_{kL}} + \frac{|v_{kL}|^2}{\omega + E_{kL}} \right) \\ &= -i \frac{\tilde{\Gamma}_{1L}}{2} \gamma_L(\omega)\end{aligned}\quad (40)$$

$$\begin{aligned}\tilde{\zeta}_{2R}(1) &= \sum_k |\tilde{h}_{2k,R}|^2 \left(\frac{|u_{kR}|^2}{\omega + E_{kR}} + \frac{|v_{kR}|^2}{\omega - E_{kR}} \right) \\ &= -i \frac{\tilde{\Gamma}_{2R}}{2} \gamma_R(\omega)\end{aligned}\quad (41)$$

$$\begin{aligned}\tilde{\zeta}_{2R}(2) &= \sum_k |\tilde{h}_{2k,R}|^2 \left(\frac{|u_{kR}|^2}{\omega - E_{kR}} + \frac{|v_{kR}|^2}{\omega + E_{kR}} \right) \\ &= -i \frac{\tilde{\Gamma}_{2R}}{2} \gamma_R(\omega)\end{aligned}\quad (42)$$

$$\begin{aligned}\tilde{\zeta}_{3L} &= \sum_k |\tilde{h}_{1k,L}|^2 v_{kL}^* u_{kL} \left(\frac{1}{\omega - E_{kL}} - \frac{1}{\omega + E_{kL}} \right) \\ &= -i \frac{\tilde{\Gamma}_{1L}}{2} \gamma_L(\omega) \frac{\Delta^*}{\omega}\end{aligned}\quad (43)$$

$$\begin{aligned}\tilde{\zeta}_{3R} &= \sum_k |\tilde{h}_{2k,R}|^2 v_{kR}^* u_{kR} \left(\frac{1}{\omega - E_{kR}} - \frac{1}{\omega + E_{kR}} \right) \\ &= -i \frac{\tilde{\Gamma}_{2R}}{2} \gamma_R(\omega) \frac{\Delta^*}{\omega}\end{aligned}\quad (44)$$

$$\begin{aligned}\tilde{\zeta}_{4L} &= \sum_k |\tilde{h}_{1k,L}|^2 v_{kL} u_{kL}^* \left(\frac{1}{\omega - E_{kL}} - \frac{1}{\omega + E_{kL}} \right) \\ &= -i \frac{\tilde{\Gamma}_{1L}}{2} \gamma_L(\omega) \frac{\Delta}{\omega}\end{aligned}\quad (45)$$

$$\begin{aligned}\tilde{\zeta}_{4R} &= \sum_k |\tilde{h}_{2k,R}|^2 v_{kR} u_{kR}^* \left(\frac{1}{\omega - E_{kR}} - \frac{1}{\omega + E_{kR}} \right) \\ &= -i \frac{\tilde{\Gamma}_{2R}}{2} \gamma_R(\omega) \frac{\Delta}{\omega}\end{aligned}\quad (46)$$

III. RESULTS and DISCUSSION

In this section, we provide a numerical study of ABSs and Josephson current, across the double quantum dots Josephson junction in T-shaped and series configurations. We discussed the behavior of ABS and Josephson current on varying the interdot tunneling and dots energy level at infinite-U limit. By equating the denominator of Eq. (21 and 38) (poles of Green's function) to zero, one can analyze the energy of subgap states ABS in T-shaped and series-configured double quantum dots Josephson junction respectively.

$$\omega - \tilde{\epsilon}_{d1} - \tilde{\Lambda} = 0 \quad (52)$$

where $\tilde{\Gamma}_{1L}$ and $\tilde{\Gamma}_{2R}$ represents the renormalized coupling strength between QD_1 with left superconducting lead and QD_2 with right superconducting lead respectively.

The mean free energy for T-shaped and series-configured double quantum dot system can be calculated by using the following formula [57]:

$$\begin{aligned}F_{MF} &= -\frac{N}{\pi} \int f(\omega) \tan^{-1} \left(\frac{\tilde{\Lambda}}{\tilde{\epsilon}_{d1} - \omega} \right) \\ &\quad + \lambda_1 (b_1^2 - 1) + \lambda_2 (b_2^2 - 1)\end{aligned}\quad (47)$$

The first term in Eq. (47) represents mean field energy for the non-interacting Anderson impurity model with renormalized parameters $(\tilde{h}_{1k,\alpha}, \tilde{h}_{2k,\alpha}, \tilde{\epsilon}_1, \tilde{\epsilon}_2, \tilde{t})$. The second and third terms result from the constraint relationship defined by Eq. (10). Now, to obtain the parameters λ_1 , λ_2 , b_1 , and b_2 we have to minimize the above equation which is done as follows.

$$\begin{aligned}\frac{\partial F_{MF}}{\partial \lambda_1} &= -\frac{N}{\pi} \int_{-D}^D \frac{f(\omega)}{(\tilde{\epsilon}_{d1} - \omega^2) + \tilde{\Lambda}^2} \left[(\tilde{\epsilon}_{d1} - \omega) \frac{\partial \tilde{\Lambda}}{\partial \lambda_1} - \tilde{\Lambda} (\tilde{\epsilon}_{d1} - \omega) \right] \\ &\quad d\omega + (b_1^2 - 1) = 0\end{aligned}\quad (48)$$

$$\begin{aligned}\frac{\partial F_{MF}}{\partial b_1} &= -\frac{N}{\pi} \int_{-D}^D \left[\frac{f(\omega)}{(\tilde{\epsilon}_{d1} - \omega^2) + \tilde{\Lambda}^2} (\tilde{\epsilon}_{d1} - \omega) \frac{\partial \tilde{\Lambda}}{\partial b_1} \right] \\ &\quad d\omega + 2\lambda_1 b_1 = 0\end{aligned}\quad (49)$$

$$\begin{aligned}\frac{\partial F_{MF}}{\partial \lambda_2} &= -\frac{N}{\pi} \int_{-D}^D \frac{f(\omega)}{(\tilde{\epsilon}_{d1} - \omega^2) + \tilde{\Lambda}^2} \left[(\tilde{\epsilon}_{d1} - \omega) \frac{\partial \tilde{\Lambda}}{\partial \lambda_2} \right] \\ &\quad d\omega + (b_2^2 - 1) = 0\end{aligned}\quad (50)$$

$$\begin{aligned}\frac{\partial F_{MF}}{\partial b_2} &= -\frac{N}{\pi} \int_{-D}^D \frac{f(\omega)}{(\tilde{\epsilon}_{d1} - \omega^2) + \tilde{\Lambda}^2} \left[(\tilde{\epsilon}_{d1} - \omega) \frac{\partial \tilde{\Lambda}}{\partial b_2} \right] \\ &\quad d\omega + 2\lambda_2 b_2 = 0\end{aligned}\quad (51)$$

Thus, from the above-coupled equations (Eq.48-Eq.51), λ_1 , λ_2 , b_1 , and b_2 can be calculated and finally the renormalized parameters $(\tilde{h}_{1k,\alpha}, \tilde{h}_{2k,\alpha}, \tilde{\epsilon}_1, \tilde{\epsilon}_2, \tilde{t})$ can be obtained for given input variables.

In the next section, we go over the numerical analysis of the Andreev bound states and Josephson current across the T-shaped and series-configured double quantum dots system for different parameters.

In Superconductor-quantum dot systems, Josephson current is carried by these subgap states. The Josephson current is calculated by differentiating the ABS with respect to the superconducting phase difference ϕ , i.e.

$$I_{SC} = \frac{\partial E_{ABS}}{\partial \phi} \quad (53)$$

We have taken all the parameters in the unit of Γ_α . For simplicity, we assume both the superconducting leads are identical i.e. $\Delta_L = \Delta_R = \Delta$ and also considered symmetric tunneling between QD 's and superconducting leads i.e. $\Gamma_L = \Gamma_R = \Gamma$.

A. T shape configuration

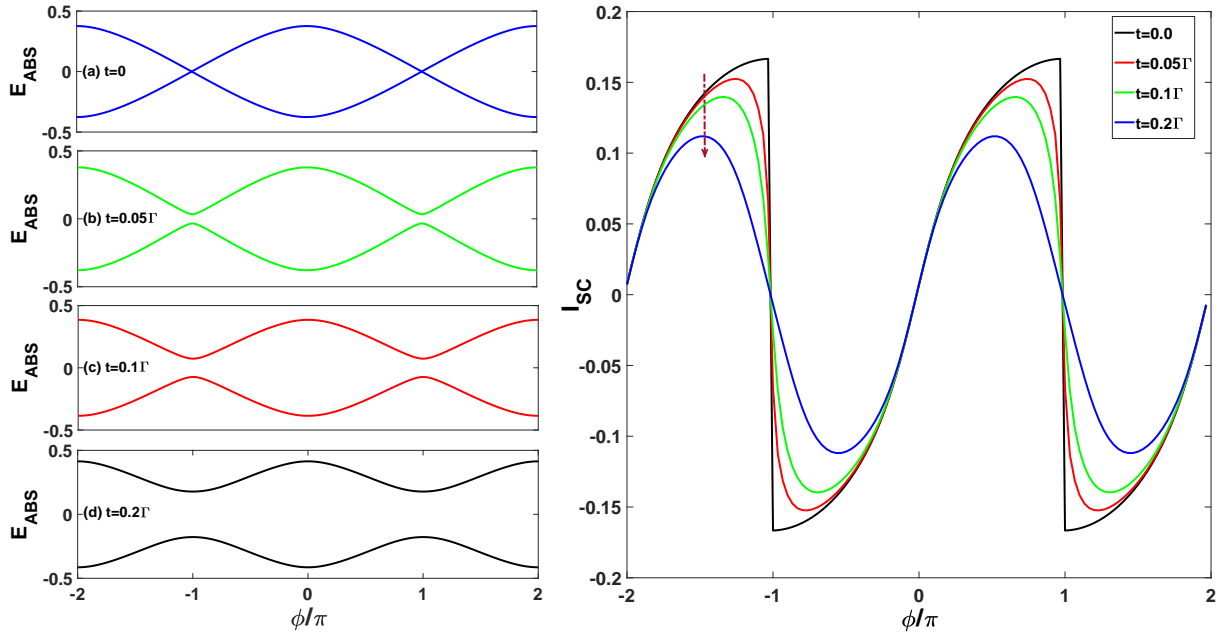


Figure 2: **left:** Energy of Andreev Bound states (E_{ABS}) and **right:** Josephson current I_{SC} (e/h) versus superconducting phase difference (ϕ) for various values of interdot tunneling. The other parameters are $\Delta = 0.5\Gamma$, $\epsilon_{d1} = \epsilon_{d2} = 0$

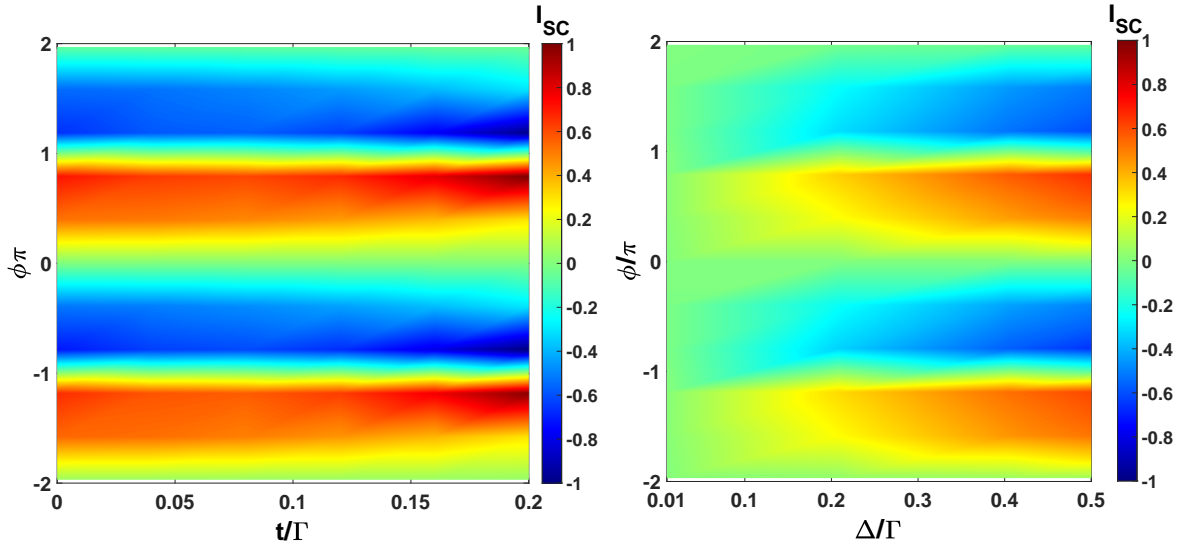


Figure 3: 2D phase diagrams of Josephson current as a function of interdot tunneling and ϕ at $\Delta/\Gamma = 0.5$ (**left**), and superconducting gap and ϕ at $t/\Gamma = 0.2$ (**right**)

In figure 2, a plot of energy of Andreev bound states (left) and Josephson current (right) versus superconducting phase difference is shown for various values of the interdot tunneling parameter (t). For $t = 0$, i.e. QD_2 is not coupled with QD_1 , the systems show the nature of the S-QD-S system. In S-QD-S systems Cooper pairs transport from one lead to another lead due to the Andreev reflection mechanism at the dot-lead interface. Here, lower and upper ABS crosses Fermi energy $E_F = 0$ and Josephson current exhibits a discontinuity at $\phi = \pm\pi$. For $t > 0$, i.e. QD_2 is coupled with QD_1 , ABS departs from Fermi energy $E_F = 0$, and Josephson current suppresses and shows sinusoidal nature. For coupled quantum dots, as t increases, the equivalent energy level ($\epsilon_{di} \pm t$) of dots splits into two, each moving away from the Fermi energy and supercurrent

suppresses. Therefore, the system does not function as a perfect transmitting channel in the case of coupled quantum dots. The explanation of suppression of Josephson current may also be stated as follows. For coupled quantum dots electrons tend to tunnel into QD_2 with increasing t . Because of this, interference destruction occurs between two transport paths, and Josephson current suppresses with increasing t . Figure 3, presents the 2D phase diagrams of Josephson current as a function of t/Γ , ϕ (left) and Δ/Γ , ϕ (right).

In figure 4, a plot of Andreev bound states (left) and Josephson current (right) versus superconducting phase difference is shown for various values of QD_1 energy levels. There is a finite gap between lower and upper ABS when energy levels of QD_1 lie above the Fermi level and Josephson current suppress with a sinusoidal nature. As the main quantum dot energy levels lie

above the Fermi level, it acts as a trap for the quasiparticles involved in Andreev reflection at the dot-lead interface. Due to this, the spectral weight of ABS reduces leading to a decrease in Josephson current. The reduction of spectral weight refers that fewer quasiparticles can tunnel into the ABSs and carry the Josephson current.

In figure 5, we plot ABS (left) and Josephson current (right) versus the superconducting phase difference for different QD_2

energy levels. The Josephson current is enhanced as the QD_2 energy levels lie above the Fermi level and suppress at the Fermi level $\epsilon_{d2} = 0$. This enhancement in Josephson current is due to the additional transport channel provided by the side dot, which increases the spectral weight of the ABS, resulting in a larger Josephson current. The gap between lower and upper ABS decreases as ϵ_{d2} departs from the Fermi level.

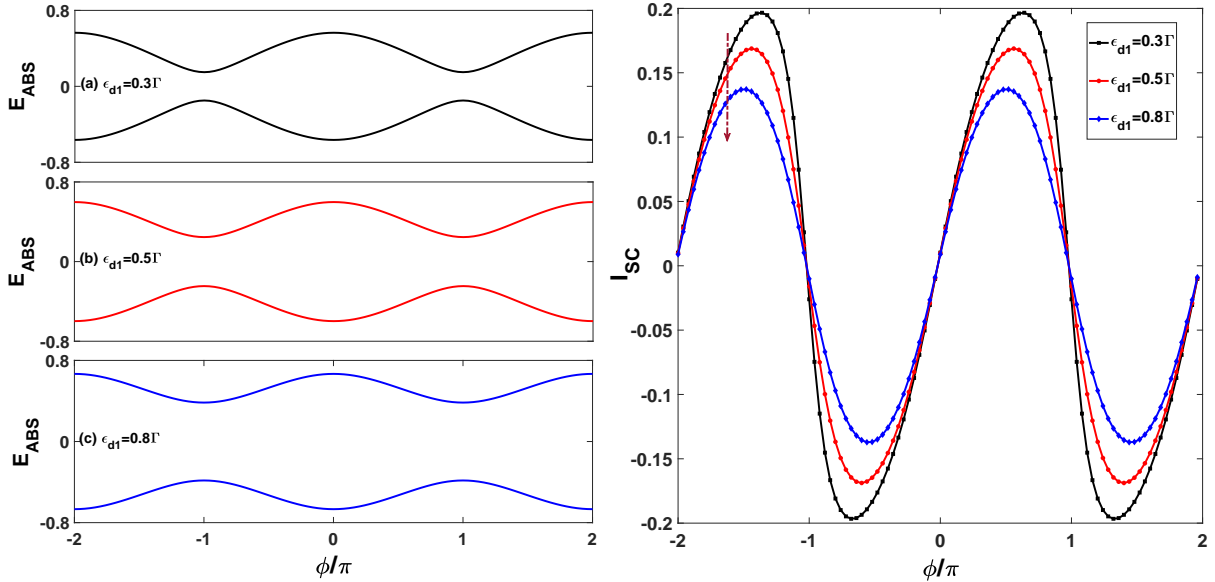


Figure 4: **left:** Energy of Andreev Bound states (E_{ABS}) versus superconducting phase difference (ϕ) for different values of QD_1 energy levels, **right:** corresponding Josephson current I_{SC} (e/h). Other parameters are $\Delta = 0.5\Gamma$, $\epsilon_{d2} = 0$, $t = 0.02\Gamma$.

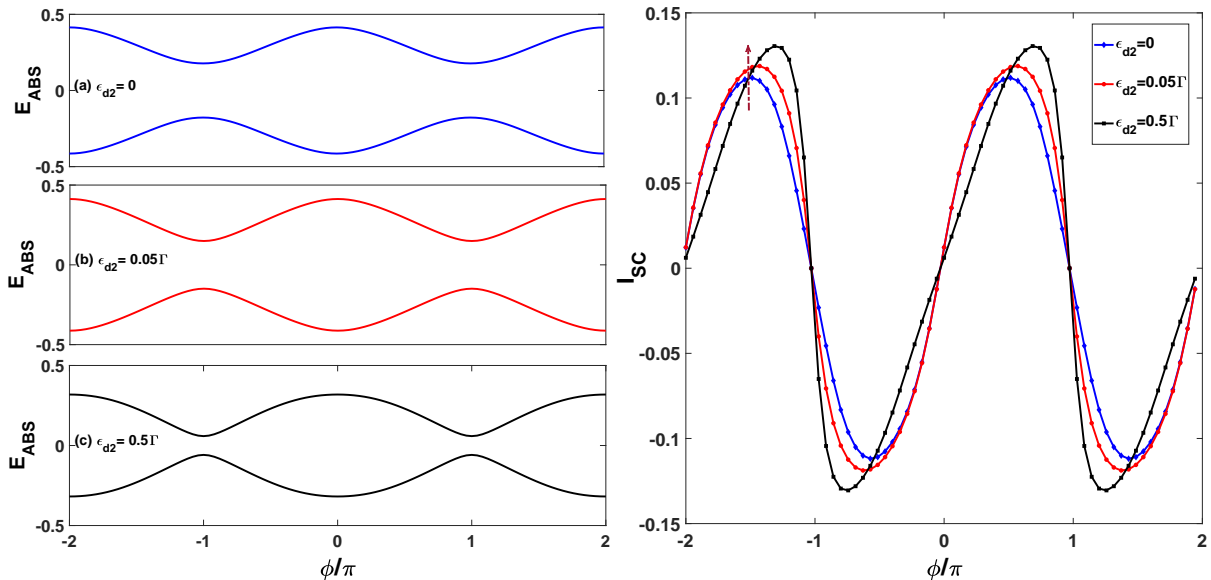


Figure 5: **left:** Energy of Andreev Bound states (E_{ABS}) and **right:** Josephson current I_{SC} (e/h) versus superconducting phase difference (ϕ) for different values of QD_2 energy levels. Other parameters are $\Delta = 0.5\Gamma$, $\epsilon_{d1} = 0$, $t = 0.2\Gamma$

B. Series configuration

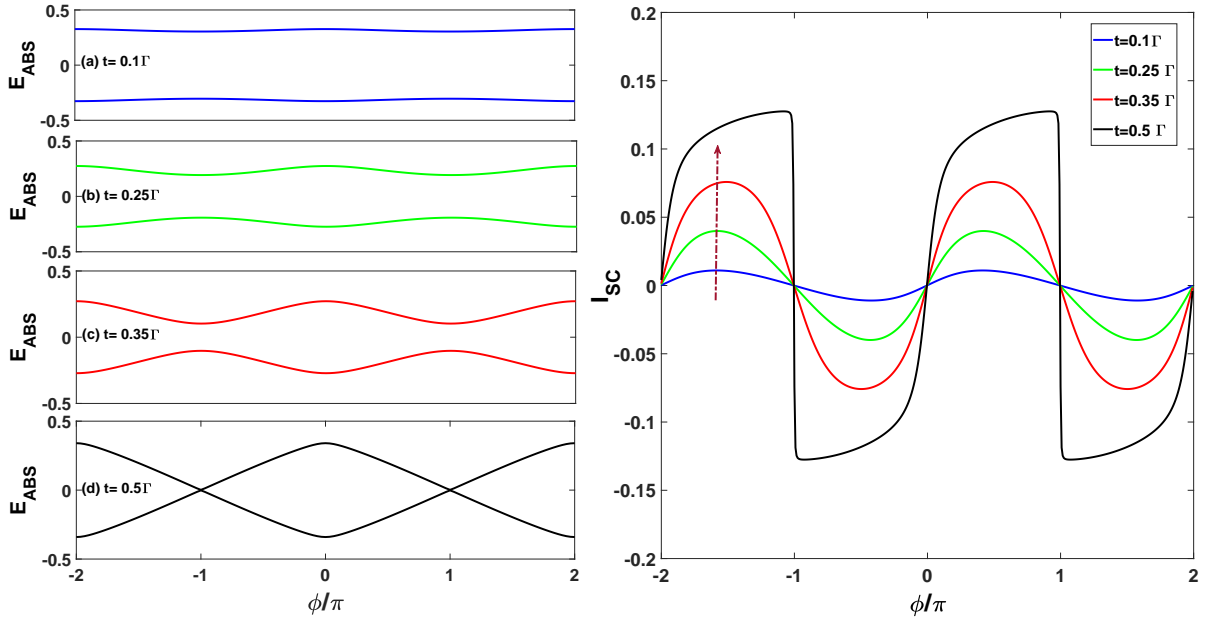


Figure 6: **left:** Energy of Andreev Bound states (E_{ABS}) and **right:** Josephson current I_{SC} (e/h) versus superconducting phase difference (ϕ) for various values of interdot tunneling. The other parameters are $\Delta = 0.5\Gamma$, $\epsilon_{d1} = \epsilon_{d2} = 0.5\Gamma$

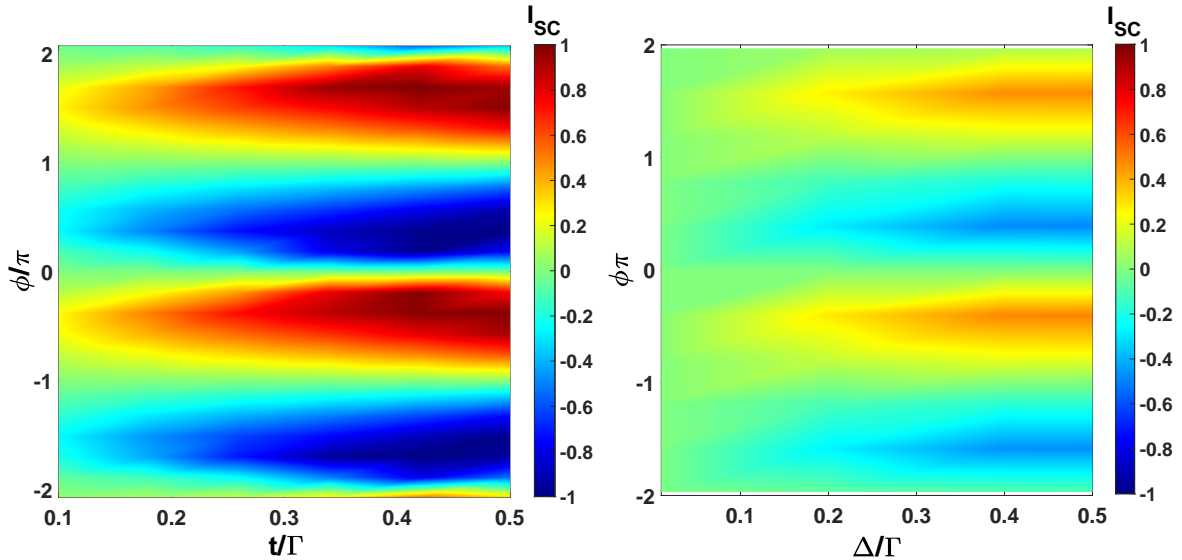


Figure 7: **left:** 2D phase diagrams of Josephson current as a function of interdot tunneling and ϕ at $\Delta/\Gamma = 0.5$ (**left**), and superconducting gap and ϕ at $t/\Gamma = 0.35$ (**right**)

In figure 6, a plot of Andreev Bound states (left) and Josephson current (right) is shown as a function of superconducting phase difference for different values of interdot tunneling. For decoupled quantum dots ($t=0$), there is no sign of ABS in the series configuration. For coupled quantum dots $t > 0$, the lower and upper ABS exhibits finite gap from Fermi energy and at $t = 0.5\Gamma$ ABS cross at Fermi energy $\omega = 0$. Further increment in t leads to a finite gap in lower and upper ABS. The supercurrent increases with increasing t and shows sinusoidal nature. For $t = 0.5\Gamma$, there is resonance tunneling between dot's energy level and lead, and the Josephson current shows a discontinuity at $\phi = \pm\pi$. The results of the series configuration are opposite from the T-shape and parallel configuration where Josephson current decreases with increasing t . Figure 7, presents the 2D phase diagrams of Josephson current as a function of $t/\Gamma, \phi$

(left) and $\Delta/\Gamma, \phi$ (right).

In figure 8, a plot of Andreev bound states (left) and Josephson current (right) versus superconducting phase difference is shown for various values of QD_1 energy levels. There is a finite gap between lower and upper ABS when energy levels of QD_1 lie above the Fermi level and cross $\omega = 0$ for $\epsilon_{d1} = 0.5$. The Josephson current increases with increasing energy levels of QD_1 and maximum for $\epsilon_{d1} = \epsilon_{d2} = 0.5$ and $t = 0.5$. With the increasing QD_1 energy levels the tunneling probability of electrons through the junction increases and thus the Josephson current increases. For the $\epsilon_{d1} = \epsilon_{d1} = t = 0.5\Gamma$ case, the resonant tunneling occurs between dots and lead, and the Josephson current is maximum.

In figure 9, we plot ABS (left) and Josephson current (right) versus the superconducting phase difference for different energy

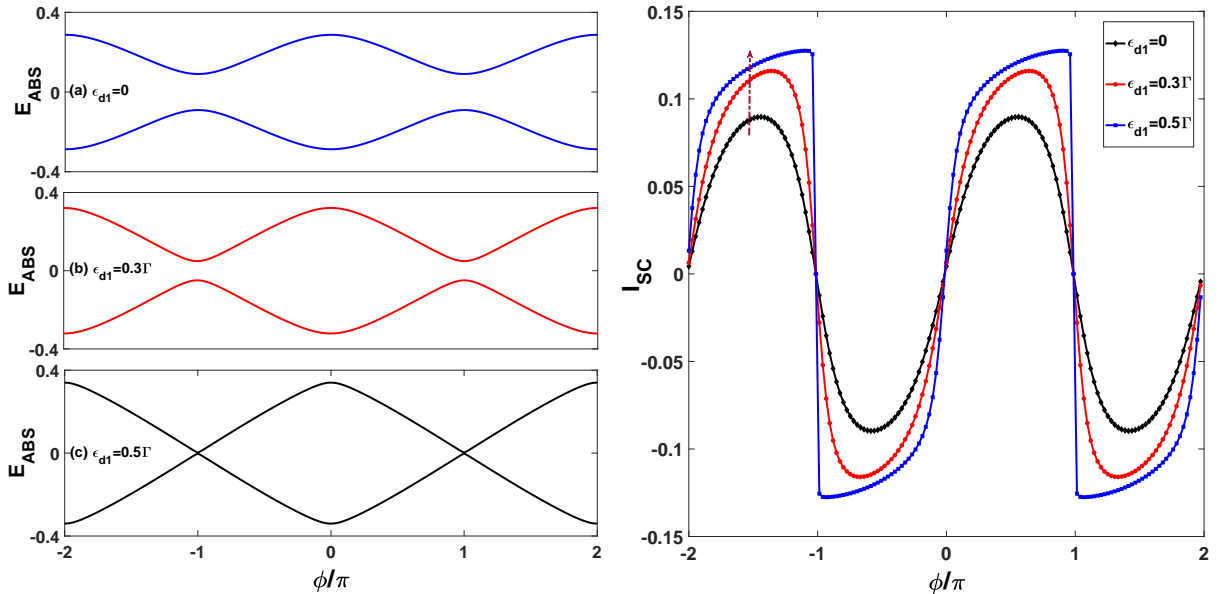


Figure 8: **left:** Energy of Andreev Bound states (E_{ABS}) versus superconducting phase difference (ϕ) for different values of QD_1 energy levels, **right:** corresponding Josephson current I_{SC} (e/h). Other parameters are $\Delta = 0.5\Gamma$, $\epsilon_{d2} = 0.5$, $t = 0.5\Gamma$.

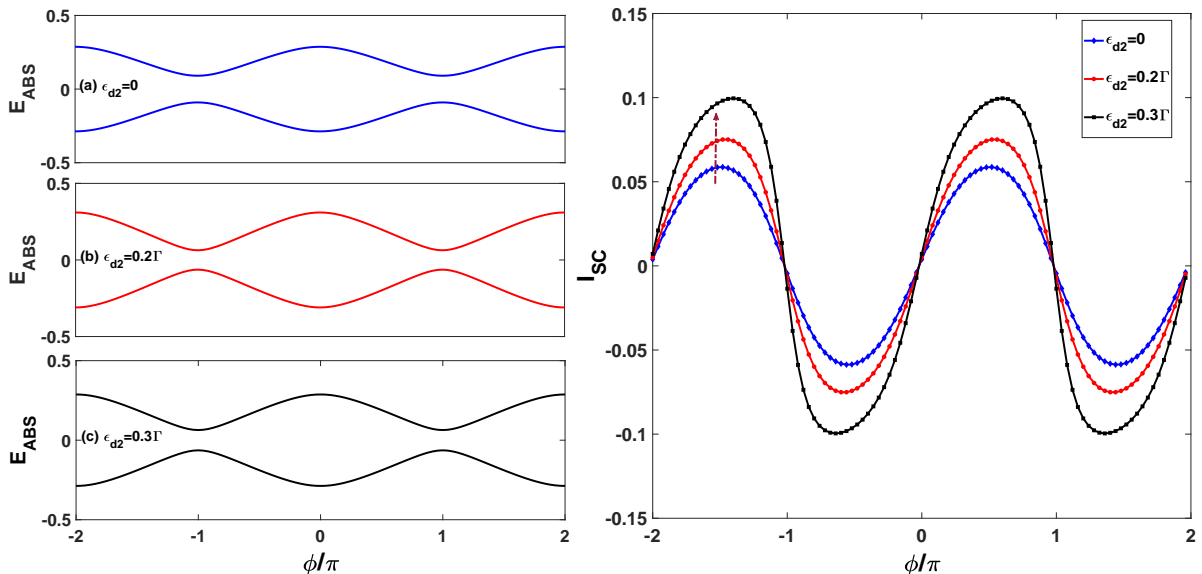


Figure 9: **left:** Energy of Andreev Bound states (E_{ABS}) and **right:** Josephson current I_{SC} (e/h) versus superconducting phase difference (ϕ) for different values of QD_2 energy levels. Other parameters are $\Delta = 0.5\Gamma$, $\epsilon_{d1} = 0.5$, $t = 0.5\Gamma$

levels of QD_2 . At the Fermi level of QD_2 ($\epsilon_{d2} = 0$), the Josephson current is suppressed, while it is enhanced as QD_2 energy levels lie above the Fermi level. The reason for the enhancement

of the Josephson current is already discussed in the previous paragraph. The gap between lower and upper ABS decreases as ϵ_{d2} departs from the Fermi level.

IV. CONCLUSION

We have addressed the Josephson transport across the double quantum dot Josephson junction in T-shape and series configuration. It is observed that interdot tunneling and energy levels of quantum dots perform a key role in the tunability of ABSs, and Josephson current. The Josephson current decreases with increasing interdot tunneling in a T-shaped configuration while enhancing in a series configuration with increasing interdot tunneling. The subgap ABS also exhibits the opposite behavior in both configurations. In T-shaped configuration, subgap ABS

cross at Fermi energy $\omega = 0$ for decoupled quantum dots and shows sinusoidal nature for coupled quantum dots. In series configuration, subgap ABS crosses Fermi energy when there is resonant tunneling between the dot's energy level i.e. $t = 0.5\Gamma$ and $\epsilon_{d1} = \epsilon_{d2} = 0.5$. We have also analyzed the nature of the energy of ABS and Josephson current with the energy levels of quantum dots for the T-shape and series configuration. As QD_1 and QD_2 energy levels rise above the Fermi level, the subgap ABS and Josephson current show different behaviors in the

T-shape configuration. The Josephson current decreases as the QD_1 energy level rises above the Fermi level, while it increases as the QD_2 energy level rises above Fermi's level. In the series configuration, the Josephson current increases as QD_1 and QD_2 energy levels lie above the Fermi level.

The study of Andreev bound states and Josephson current can be useful in quantum computing and nanoelectronics. Controlling the Andreev bound states and Josephson current in dou-

ble quantum dot-based Josephson junctions may improve the efficiency and robustness of quantum processing [65]. Josephson junctions are key building blocks of superconducting electronics, which have extensive uses in sensing, metrology, and communication. The double quantum dot-based Josephson junction could offer tunable supercurrents and novel noise properties in future superconducting devices [66–69]. This study can also be extended for multi-dot and multi-terminal Josephson junctions.

Acknowledgement Authors offer their gratitude to the DST-SER-1644-PHY 2021-22 research project for financial support. Bhupendra Kumar, a research scholar in the Department

of Physics, IIT Roorkee, also acknowledges the support from the Ministry of Education (MoE), India in the form of a Ph.D. fellowship.

References

- [1] B. D. Josephson, Possible new effects in superconductive tunnelling, *Physics Letters* 1 (1962) 251–253. doi:10.1016/0031-9163(62)91369-0.
- [2] P. W. Anderson, How josephson discovered his effect, *Phys. Today* 23 (11) (1970) 23–29. doi:10.1063/1.3021826.
- [3] Kouwenhoven, et al., Few-electron quantum dots, *Reports on Progress in Physics* 64 (6) (2001) 701. doi:10.1088/0034-4885/64/6/201.
- [4] M. A. Kastner, Artificial atoms, *Physics Today* 46 (1993). doi:10.1063/1.881393.
- [5] A. Martín-Rodero, A. Levy Yeyati, Josephson and andreev transport through quantum dots, *Advances in Physics* 60 (6) (2011) 899–958. doi:10.1038/nnano.2010.173.
- [6] D. Franceschi, et al., Hybrid superconductor–quantum dot devices, *Nature nanotechnology* 5 (10) (2010) 703–711. doi:10.1038/nnano.2010.173.
- [7] Eichler, et al., Even-odd effect in andreev transport through a carbon nanotube quantum dot, *Phys. Rev. Lett.* 99 (2007) 126602. doi:10.1103/PhysRevLett.99.126602.
- [8] M. R. Buitelaar, et al., Quantum dot in the kondo regime coupled to superconductors, *Phys. Rev. Lett.* 89 (2002) 256801. doi:10.1103/PhysRevLett.89.256801.
- [9] T. Sand-Jespersen, et al., Kondo-enhanced andreev tunneling in inas nanowire quantum dots, *Physical review letters* 99 (12) (2007) 126603. doi:10.1103/PhysRevLett.99.126603.
- [10] K. G. Rasmussen, et al., Kondo resonance enhanced supercurrent in single wall carbon nanotube josephson junctions, *New Journal of Physics* 9 (2007). doi:10.1088/1367-2630/9/5/124.
- [11] J. P. Cleuziou, et al., Carbon nanotube superconducting quantum interference device, *Nature Nanotechnology* 1 (2006). doi:10.1038/nnano.2006.54.
- [12] R. Maurand, et al., First-order $0 - \pi$ quantum phase transition in the kondo regime of a superconducting carbon-nanotube quantum dot, *Phys. Rev. X* 2 (2012) 011009. doi:10.1103/PhysRevX.2.011009.
- [13] J. A. V. Dam, et al., Supercurrent reversal in quantum dots, *Nature* 442 (2006). doi:10.1038/nature05018.
- [14] S. Verma, Ajay, Influence of superconductivity on the magnetic moment of quantum impurity embedded in bcs superconductor, *Journal of Physics Condensed Matter* 33 (2020). doi:10.1088/1361-648X/abcc0e.
- [15] Buitelaar, et al., Multiple andreev reflections in a carbon nanotube quantum dot, *Phys. Rev. Lett.* 91 (2003) 057005. doi:10.1103/PhysRevLett.91.057005.
- [16] P. Jarillo-Herrero, et al., Quantum supercurrent transistors in carbon nanotubes, *Nature* 439 (2006). doi:10.1038/nature04550.
- [17] H. I. Jørgensen, et al., Electron transport in single-wall carbon nanotube weak links in the fabry-perot regime, *Phys. Rev. Lett.* 96 (2006) 207003. doi:10.1103/PhysRevLett.96.207003.
- [18] J. H. Ingerslev, et al., Critical current $0 - \pi$ transition in designed josephson quantum dot junctions, *Nano Letters* 7 (8) (2007) 2441–2445. doi:10.1021/nl071152w.
- [19] H. I. Jørgensen, et al., Critical and excess current through an open quantum dot: Temperature and magnetic-field dependence, *Phys. Rev. B* 79 (2009) 155441. doi:10.1103/PhysRevB.79.155441.
- [20] J. D. Pillet, et al., Andreev bound states in supercurrent-carrying carbon nanotubes revealed, *Nature Physics* 6 (2010). doi:10.1038/nphys1811.

- [21] L. Hofstetter, et al., Cooper pair splitter realized in a two-quantum-dot y-junction, *Nature* 461 (2009). [doi:10.1038/nature08432](https://doi.org/10.1038/nature08432).
- [22] L. G. Herrmann, et al., Carbon nanotubes as cooper-pair beam splitters, *Phys. Rev. Lett.* 104 (2010) 026801. [doi:10.1103/PhysRevLett.104.026801](https://doi.org/10.1103/PhysRevLett.104.026801).
- [23] E. Vecino, et al., Josephson current through a correlated quantum level: Andreev states and π junction behavior, *Physical Review B* 68 (3) (2003) 035105. [doi:10.1103/PhysRevB.68.035105](https://doi.org/10.1103/PhysRevB.68.035105).
- [24] M.-S. Choi, et al., Kondo effect and josephson current through a quantum dot between two superconductors, *Physical Review B* 70 (2) (2004) 020502. [doi:10.1103/PhysRevB.70.020502](https://doi.org/10.1103/PhysRevB.70.020502).
- [25] J. S. Lim, et al., Andreev bound states in the kondo quantum dots coupled to superconducting leads, *Journal of Physics: Condensed Matter* 20 (41) (2008) 415225. [doi:10.1088/0953-8984/20/41/415225](https://doi.org/10.1088/0953-8984/20/41/415225).
- [26] Y. Zhu, et al., Andreev bound states and the π -junction transition in a superconductor/quantum-dot/superconductor system, *Journal of Physics: Condensed Matter* 13 (39) (2001) 8783. [doi:10.1088/0953-8984/13/39/307](https://doi.org/10.1088/0953-8984/13/39/307).
- [27] K. Christoph, et al., Josephson current through a single anderson impurity coupled to bcs leads, *Physical Review B* 77 (2) (2008) 024517. [doi:10.1103/PhysRevB.77.024517](https://doi.org/10.1103/PhysRevB.77.024517).
- [28] S. guang Cheng, Q. feng Sun, Josephson current transport through t-shaped double quantum dots, *Journal of Physics: Condensed Matter* 20 (50) (2008) 505202. [doi:10.1088/0953-8984/20/50/505202](https://doi.org/10.1088/0953-8984/20/50/505202).
- [29] L. Rosa, et al., Josephson current through a kondo molecule, *Phys. Rev. B* 75 (2007) 045132. [doi:10.1103/PhysRevB.75.045132](https://doi.org/10.1103/PhysRevB.75.045132).
- [30] Ortega-Taberner, et al., Anomalous josephson current through a driven double quantum dot, *Phys. Rev. B* 107 (2023) 115165. [doi:10.1103/PhysRevB.107.115165](https://doi.org/10.1103/PhysRevB.107.115165).
- [31] F. Chi, S. S. Li, Current-voltage characteristics in strongly correlated double quantum dots, *Journal of Applied Physics* 97 (2005). [doi:10.1063/1.1939065](https://doi.org/10.1063/1.1939065).
- [32] Z. Yu, et al., Probing spin states of coupled quantum dots by a dc josephson current, *Phys. Rev. B* 66 (2002) 085306. [doi:10.1103/PhysRevB.66.085306](https://doi.org/10.1103/PhysRevB.66.085306).
- [33] S. Droste, et al., Josephson current through interacting double quantum dots with spin-orbit coupling, *Journal of Physics Condensed Matter* 24 (2012). [doi:10.1088/0953-8984/24/41/415301](https://doi.org/10.1088/0953-8984/24/41/415301).
- [34] G. Rajput, R. Kumar, Ajay, Tunable josephson effect in hybrid parallel coupled double quantum dot-superconductor tunnel junction, *Superlattices and Microstructures* 73 (2014) 193–202. [doi:https://doi.org/10.1016/j.spmi.2014.05.029](https://doi.org/10.1016/j.spmi.2014.05.029).
- [35] R. Žitko, et al., Josephson current in strongly correlated double quantum dots, *Phys. Rev. Lett.* 105 (2010) 116803. [doi:10.1103/PhysRevLett.105.116803](https://doi.org/10.1103/PhysRevLett.105.116803).
- [36] J. C. E. Saldaña, et al., Supercurrent in a double quantum dot, *Physical Review Letters* 121 (2018). [doi:10.1103/PhysRevLett.121.257701](https://doi.org/10.1103/PhysRevLett.121.257701).
- [37] H. Haug, A.-P. Jauho, et al., *Quantum kinetics in transport and optics of semiconductors*, Vol. 2, Springer, Berlin, 2008. [doi:10.1007/978-3-540-73564-9](https://doi.org/10.1007/978-3-540-73564-9).
- [38] L. V. Keldysh, et al., Diagram technique for nonequilibrium processes, *Sov. Phys. JETP* 20 (4) (1965) 1018–1026.
- [39] D. J. Luitz, et al., Understanding the josephson current through a kondo-correlated quantum dot, *Phys. Rev. Lett.* 108 (2012) 227001. [doi:10.1103/PhysRevLett.108.227001](https://doi.org/10.1103/PhysRevLett.108.227001).
- [40] B. Probst, et al., Signatures of nonlocal cooper-pair transport and of a singlet-triplet transition in the critical current of a double-quantum-dot josephson junction, *Physical Review B* 94 (2016). [doi:10.1103/PhysRevB.94.155445](https://doi.org/10.1103/PhysRevB.94.155445).
- [41] B. Sothmann, et al., Josephson response of a conventional and a noncentrosymmetric superconductor coupled via a double quantum dot, *Phys. Rev. B* 92 (2015) 014504. [doi:10.1103/PhysRevB.92.014504](https://doi.org/10.1103/PhysRevB.92.014504).
- [42] X. Q. Wang, G. Y. Yi, W. J. Gong, Effect of interdot coulomb interaction on the josephson phase transition in a double-quantum-dot junction, *Superlattices and Microstructures* 109 (2017). [doi:10.1016/j.spmi.2017.05.026](https://doi.org/10.1016/j.spmi.2017.05.026).
- [43] M.-S. Choi, et al., Spin-dependent josephson current through double quantum dots and measurement of entangled electron states, *Phys. Rev. B* 62 (2000) 13569–13572. [doi:10.1103/PhysRevB.62.13569](https://doi.org/10.1103/PhysRevB.62.13569).
- [44] J. F. Rentrop, et al., Nonequilibrium transport through a josephson quantum dot, *Phys. Rev. B* 89 (2014) 235110. [doi:10.1103/PhysRevB.89.235110](https://doi.org/10.1103/PhysRevB.89.235110).
- [45] T. Domański, et al., Josephson-phase-controlled interplay between correlation effects and electron pairing in a three-terminal nanostructure, *Phys. Rev. B* 95 (2017) 045104. [doi:10.1103/PhysRevB.95.045104](https://doi.org/10.1103/PhysRevB.95.045104).

- [46] K. Grove-Rasmussen, et al., Yu-shiba-rusinov screening of spins in double quantum dots, *Nature Communications* 9 (2018). doi:[10.1038/s41467-018-04683-x](https://doi.org/10.1038/s41467-018-04683-x).
- [47] S. Baba, et al., Gate tunable parallel double quantum dots in inas double-nanowire devices, *Applied Physics Letters* 111 (2017). doi:[10.1063/1.4997646](https://doi.org/10.1063/1.4997646).
- [48] A. Y. Kasumov, et al., Proximity effect in a superconductor-metallofullerene-superconductor molecular junction, *Phys. Rev. B* 72 (2005) 033414. doi:[10.1103/PhysRevB.72.033414](https://doi.org/10.1103/PhysRevB.72.033414).
- [49] W. G. van der Wiel, et al., Electron transport through double quantum dots, *Rev. Mod. Phys.* 75 (2002) 1–22. doi:[10.1103/RevModPhys.75.1](https://doi.org/10.1103/RevModPhys.75.1).
- [50] M. Nilsson, et al., Parallel-coupled quantum dots in inas nanowires, *Nano Letters* 17 (2017). doi:[10.1021/acs.nanolett.7b04090](https://doi.org/10.1021/acs.nanolett.7b04090).
- [51] H. I. Jørgensen, et al., Critical current $0 - \pi$ transition in designed josephson quantum dot junctions, *Nano Letters* 7 (2007). doi:[10.1021/nl071152w](https://doi.org/10.1021/nl071152w).
- [52] P. Zhang, et al., Signatures of andreev blockade in a double quantum dot coupled to a superconductor, *Phys. Rev. Lett.* 128 (2022) 046801. doi:[10.1103/PhysRevLett.128.046801](https://doi.org/10.1103/PhysRevLett.128.046801).
- [53] Y. Avishai, et al., Superconductor-quantum dot-superconductor junction in the kondo regime, *Phys. Rev. B* 67 (2003) 041301. doi:[10.1103/PhysRevB.67.041301](https://doi.org/10.1103/PhysRevB.67.041301).
- [54] A. L. Yeyati, et al., Nonequilibrium dynamics of andreev states in the kondo regime, *Phys. Rev. Lett.* 91 (2003) 266802. doi:[10.1103/PhysRevLett.91.266802](https://doi.org/10.1103/PhysRevLett.91.266802).
- [55] R. S. Deacon, et al., Cooper pair splitting in parallel quantum dot josephson junctions, *Nature Communications* 6 (2015). doi:[10.1038/ncomms8446](https://doi.org/10.1038/ncomms8446).
- [56] P. Coleman, New approach to the mixed-valence problem, *Phys. Rev. B* 29 (1984) 3035–3044. doi:[10.1103/PhysRevB.29.3035](https://doi.org/10.1103/PhysRevB.29.3035).
- [57] P. Coleman, Large n as a classical limit $\frac{1}{N} \approx \exists$ of mixed valence, *J. Magn. Magn. Mater* 47 (48) (1985) 323.
- [58] M. Lavagna, A. J. Millis, P. A. Lee, d -wave superconductivity in the large-degeneracy limit of the anderson lattice, *Phys. Rev. Lett.* 58 (1987) 266–269. doi:[10.1103/PhysRevLett.58.266](https://doi.org/10.1103/PhysRevLett.58.266).
- [59] G. Kotliar, A. E. Ruckenstein, New functional integral approach to strongly correlated fermi systems: The gutzwiller approximation as a saddle point, *Phys. Rev. Lett.* 57 (1986) 1362–1365. doi:[10.1103/PhysRevLett.57.1362](https://doi.org/10.1103/PhysRevLett.57.1362).
- [60] P. Schwab, R. Raimondi, Andreev tunneling in quantum dots: A slave-boson approach, *Phys. Rev. B* 59 (1999) 1637–1640. doi:[10.1103/PhysRevB.59.1637](https://doi.org/10.1103/PhysRevB.59.1637).
- [61] T. Chamoli, Ajay, Josephson transport through parallel double coupled quantum dots at infinite- u limit, *The European Physical Journal B* 95 (9) (2022) 163. doi:<https://doi.org/10.1007/s10948-021-06002-w>.
- [62] T. Chamoli, Ajay, Andreev bound states in superconductor–quantum dot–superconductor junction at infinite- u limit, *Journal of Superconductivity and Novel Magnetism* 35 (2022). doi:[10.1007/s10948-021-06002-w](https://doi.org/10.1007/s10948-021-06002-w).
- [63] B.-K. Kim, et al., Transport measurement of andreev bound states in a kondo-correlated quantum dot, *Phys. Rev. Lett.* 110 (2013) 076803. doi:[10.1103/PhysRevLett.110.076803](https://doi.org/10.1103/PhysRevLett.110.076803).
- [64] J. O. Island, et al., Proximity-induced shiba states in a molecular junction, *Phys. Rev. Lett.* 118 (2017) 117001. doi:[10.1103/PhysRevLett.118.117001](https://doi.org/10.1103/PhysRevLett.118.117001).
- [65] G. Wendin, V. Shumeiko, Quantum bits with josephson junctions, *Low Temperature Physics* 33 (9) (2007) 724–744. doi:<https://doi.org/10.1063/1.2780165>.
- [66] Arnault, et al., Dynamical stabilization of multiplet supercurrents in multiterminal josephson junctions, *Nano Letters* 22 (17) (2022) 7073–7079. doi:<https://doi.org/10.1021/acs.nanolett.2c01999>.
- [67] G.-Y. Yi, et al., Suppression of the $0 - \pi$ transition in a josephson junction with parallel double-quantum-dot barriers, *Phys. Rev. B* 98 (2018) 035438. doi:[10.1103/PhysRevB.98.035438](https://doi.org/10.1103/PhysRevB.98.035438).
- [68] A. Vekris, et al., Josephson junctions in double nanowires bridged by in-situ deposited superconductors, *Phys. Rev. Res.* 3 (2021) 033240. doi:[10.1103/PhysRevResearch.3.033240](https://doi.org/10.1103/PhysRevResearch.3.033240).
- [69] A. Bargerbos, et al., Singlet-doublet transitions of a quantum dot josephson junction detected in a transmon circuit, *PRX Quantum* 3 (2022) 030311. doi:[10.1103/PRXQuantum.3.030311](https://doi.org/10.1103/PRXQuantum.3.030311).